BMB Reports - Manuscript Submission

Manuscript Draft

DOI: 10.5483/BMBRep.2022-0137

Manuscript Number: BMB-22-137

Title: Preventive effects of nano-graphene oxide against Parkinson's disease via reactive oxygen species scavenging and anti-inflammation

Article Type: Article

Keywords: 6-hydroxydopamine; forelimb akinesia; nano-graphene oxide; Parkinson; reactive oxygen species

Corresponding Author: Hyung Ho Yoon

Authors: Hyung Ho Yoon[1,*,#], Hee-Yeong Kim[2,#], Hanyu Seong[3,#], Dong Kwang Seo[1], Soon Won Choi[2,4], Kyung-Sun Kang[2], Sang Ryong Jeon[1]

Institution: [1]Department of Neurological Surgery, Asan Medical Center,
[2]Adult Stem Cell Research Center and Research Institute for Veterinary Science, Seoul National University,
[3]Department of Neurosurgery, Seoul Bumin Hospital,
[4]Institute of Bio & Nano Convergence, Biogo Co.,

Manuscript Type: Article

Title: Preventive effects of nano-graphene oxide against Parkinson's disease via reactive oxygen species scavenging and anti-inflammation

Author's name: Hee-Yeong Kim[a*], Hyung Ho Yoon[b*], Hanyu Seong[c*], Dong Kwang Seo[b], Soon Won Choi[a,d], Kyung-Sun Kang[a†], Sang Ryong Jeon[b†]

Affiliation: [a]Adult Stem Cell Research Center and Research Institute for Veterinary Science, College of Veterinary Medicine, Seoul National University, Seoul 08826, Republic of Korea

[b]Department of Neurological Surgery, Asan Medical Center, University of Ulsan College of Medicine, Seoul 05505, Korea

[c]Department of Neurosurgery, Seoul Bumin Hospital, Seoul 07590, Republic of Korea

[d]Institute of Bio & Nano Convergence, Biogo Co., LTD, Seoul 08826, Republic of Korea

*These authors contributed equally to this work.

Running Title: daNGO protects dopaminergic neurons

Keywords: 6-hydroxydopamine; forelimb akinesia; nano-graphene oxide; Parkinson's disease; reactive oxygen species.

†**Corresponding Author's Information:** Sang Ryong Jeon, M.D., Ph.D. Tel: +82-2-3010-3562, E-mail: srjeon@amc.seoul.kr and Kyung-Sun Kang, DVM., Ph.D. Tel: +82-2-880-1246, E-mail: kangpub@snu.ac.kr

ABSTRACT

We investigated the neuroprotective effects of deca nano-graphene oxide (daNGO) against reactive oxygen species (ROS) and inflammation in the human neuroblastoma cell line SH-SY5Y and in the 6-hydroxydopamine (6-OHDA) induced Parkinsonian rat model. An MTT assay was performed to measure cell viability *in vitro* in the presence of 6-OHDA and/or daNGO. The intracellular ROS level was quantified using 2′,7′-dichlorofluorescein diacetate. daNGO showed neuroprotective effects against 6-OHDA-induced toxicity and also displayed ROS scavenging properties. We then tested the protective effects of daNGO against 6-OHDA induced toxicity in a rat model. Stepping tests showed that the akinesia symptoms were improved in the daNGO group compared to the control group. Moreover, in an apomorphine-induced rotation test, the number of net contralateral rotations was decreased in the daNGO group compared to the control group. By immunofluorescent staining, the animals in the daNGO group had more tyrosine hydroxylase-positive cells than the controls. By anti-Iba1 staining, 6-OHDA induced microglial activation showed a significantly decrease in the daNGO group, indicating that the neuroprotective effects of graphene resulted from anti-inflammation. In conclusion, nano-graphene oxide has neuroprotective effects against the neurotoxin induced by 6-OHDA on dopaminergic neurons.

INTRODUCTION

Parkinson's disease (PD) is a neurodegenerative disorder characterized by the progressive loss of dopaminergic neurons in the substantia nigra (SN). The cardinal symptoms of PD include resting tremor, rigidity, and bradykinesia (1). The most common treatment for this condition is L-3,4-dihydroxyphenylalanine (L-DOPA), a precursor of dopamine, which can improve the motor symptoms of affected patients. However, as the loss of dopaminergic neurons gradually progresses, motor complications such as L-DOPA-induced dyskinesias, wearing-off, and motor fluctuations may occur (2). Electrical deep brain stimulation (DBS) has been widely used to alleviate these symptoms in advanced PD patients (3).

There is currently no approved treatment that blocks or modulates the progression of PD. It is still therefore necessary to develop new disease-modifying therapies based on the pathophysiology of PD as an alternative to the existing dopamine-dependent treatments (4). In the pathogenesis of PD, among the most important disease causes are neuroinflammation and oxidative stress (5, 6). Graphene oxide (GO) has thus emerged as a possible candidate treatment for PD as it can suppress both of these processes (7, 8). Graphene quantum dots (GQD), which are graphene fragments of less than 20 nm in diameter (9), have been demonstrated to have biocompatibility and anti-inflammatory effects in patients with colitis (7). Moreover, GQDs have been shown to dissociate α-synuclein fibril by decreasing β-sheet structure, thereby preventing dopaminergic neuronal loss by reducing α-synuclein toxicity (10). However, the effects of GO on mitochondria can be both beneficial and detrimental. GO protects neuroblastoma cells against the prion-mediated mitochondrial toxicity via an autophagic flux (11). By contrast however, GO-induced reactive oxygen species (ROS) can disrupt mitochondrial homeostasis (12). Since the effects of GO greatly depend on its size (13-16), we manufactured GO with a 10 nm lateral size on average to minimize the possible induction of oxidative stress. We termed these deca nano-graphene oxide (daNGO). We here

describe our investigation of the neuroprotective effects of the daNGO against ROS and inflammation in the human neuroblastoma cell line SH-SY5Y and *in vivo* in the 6-hydroxydopamine (6-OHDA) induced Parkinsonian rat model.

RESULTS

Characterization of the deca nano-graphene oxide

daNGOs were synthesized using a modified Taylor method to obtain a single- or few-layers of graphene oxide with high oxidation efficiency (Fig. 1A). The lateral size of the daNGO particles was determined using a particle size analyzer (PSA) and was found to vary from 5 to 25 nm. The vast majority (99%) of the particles were less than 18.2 nm in size, and 50% of the distributed particles showed a size of 10.1 ± 7.3 nm. These data indicated that the average lateral size of the daNGOs was 10 nm (Fig. 1B). Images and the height profile of the daNGOs were characterized using AFM analysis. AFM images of 4 μm^2 indicated a nanoparticle with the height of 1.44 ± 0.14 nm (Fig. 1C, D). These results suggested that the daNGOs were composed of a single- or few layer graphene oxides of a nanoscale diameter.

daNGOs protect SH-SY5Y cells against 6-OHDA-induced neurotoxicity

An *in vitro* MTT assay was performed to determine the level of cytotoxicity generated by 6-OHDA and to verify the neuronal protective effects of daNGO. SH-SY5Y cells were treated with 6-OHDA (5-400 μM) and/or daNGO (300 ng/ml - 60 μg/ml) for 24 hours. Treatment with 6-OHDA alone decreased the cell viability in concentration-dependent manner but there was no significant change in cell viability upon exposure to various daNGO doses (Fig. 2B, C). When the cells were treated with both 6-OHDA and daNGO, the cell viability

significantly increased as the concentration of daNGO increased compared to the cells treated with 6-OHDA only (Fig. 2D; *$P < 0.05$; ***$P < 0.001$).

daNGOs scavenge 6-OHDA-induced ROS in SH-SY5Y cells

It has been reported previously that 6-OHDA increases the intracellular oxidative stress level through ROS production in SH-SY5Y cells (17). To investigate the protective effects of daNGOs against oxidative stress caused by scavenging ROS, we measured the intracellular ROS levels using a DCF-DA assay in 6-OHDA-treated SH-SY5Y cells. The cells were stained with DCF-DA and analyzed using FACS equipment. Exposure of the cells to 6-OHDA increased the ROS level as compared with the control group. However, co-treatment with both 6-OHDA and daNGO significantly decreased the ROS level compared with the control group and 6-OHDA only group (Fig. 2E, F; **$P < 0.01$; ***$P < 0.001$).

daNGOs improve the symptoms of forelimb akinesia

We conducted *in vivo* analyses of the effects of daNGOs in a rat model of PD. daNGOs (30mg/kg, 5 days, i.p.) were injected into the animals immediately after 6-OHDA injection. All the rats in the PD control group showed considerable contralateral forelimb akinesia in stepping tests (Fig. 3B, D). In contrast, this symptom was significantly improved in the daNGO group (Fig. 3B, D; ***$P < 0.001$). These beneficial effects of the daNGOs persisted two weeks after 6-OHDA injection (Fig. 3B, D). No effect of a unilateral 6-OHDA injection was seen on the number of ipsilateral forelimb steps in any of the rats (Fig. 3C).

daNGOs alleviate apomorphine-induced rotation

Apomorphine-induced rotation tests were performed in the PD model rats at 7 days after 6-

OHDA injections. The daNGO group showed a significant decrease in net (contra-ipsi) rotations per minute compared with the PD control group (Fig. 3E; $*P < 0.05$). In the 5 min interval record, the number of net rotations decreased significantly in the daNGO group until 15 minutes after apomorphine injection compared with the PD control group (Fig. 3F; $*P < 0.05$; $**P < 0.01$).

daNGOs protect dopaminergic neurons from 6-OHDA-induced neuroinflammation

Immunofluorescent staining of sections of lesioned SNs from the PD rat model revealed a considerable loss of tyrosine hydroxylase (TH)-positive cells in the PD control group (-87.4 ± 1.8%; Fig. 4A) compared with the daNGO group (-67.9 ± 3.6%; Fig. 4B). There were significant differences found between these two groups ($**P < 0.01$, $*P < 0.05$; Fig. 4C, D). We next conducted anti-Iba-1 staining to explore whether the daNGOs modulated 6-OHDA-induced neuroinflammation. The results indicated a significant decrease in the large size of the Iba-1 positive cells of ipsilateral SN in the daNGO group compared with the PD control group, meaning that the number of activated microglia (which have an increased cell body) was decreased in the daNGO group ($*P < 0.05$; Fig. 4E).

DISCUSSION

GO is a promising therapeutic agent that consists of oxidizing graphite carbon atoms (18). It has a large surface area, contains functional groups, and has a high biocompatibility, which can be used as a drug carrier in cancer therapy (19, 20). Graphene nanostructures can also cross the blood brain barrier (21) and thereby provide a highly efficient delivery to targeted brain areas. Regarding the pathophysiology of PD, ROS- and glial cell-induced neuroinflammation are known to be principal factors in the generation of sporadic PD (22). In

the current literature, ROS have been reported to also induce mitochondrial dysfunction and oxidative stress (23). In previous studies, GQD was demonstrated to have anti-inflammatory effects against colitis, and we expected that it would exert these same effects in the brain as it can cross the blood-brain barrier (13). In addition to this, GO quantum dots (lateral sizes, 20-40nm) can reduce the ROS level and exert neuroprotective effects (24). However, some studies have also reported that GO can produce ROS and oxidative stress, causing cytotoxicity (25-27). Previous studies have shown that larger GOs (lateral sizes, 750-1300nm) increased macrophages and induced stronger inflammation (14, 15). In contrast, smaller GOs showed a high potential for ROS scavenging (16). Moreover, nanoscale GO had great anti-oxidant and anti-inflammatory effects in vivo (13, 24). Hence, we chose to use nanoscale GO in this study. We consider therefore that the opposing functions of GO regarding neuroprotective and neurotoxic effects are dependent on size i.e. nanoscale GO particles have ROS scavenging and neuroprotection characteristics whereas a larger GO size has contrary effects. In addition, GO size could be a crucial factor to enhance GO permeability across the blood-brain barrier (10). In our current study, we manufactured nanosized GO, which we termed daNGOs due to the 10nm lateral size of these particles on average. To evaluate the potential neuroprotective, anti-neuroinflammatory, and ROS reducing effects of the daNGOs, we used 6-OHDA and the neuroblastoma cell line SH-SY5Y. 6-OHDA is a neurotoxin that specifically destroys dopaminergic neurons by causing oxidative stress and inflammation (28). SH-SY5Y cells are widely used and thus well established in PD studies (29). In these initial *in vitro* experiments, we found that daNGO treatments had neuroprotective effects against 6-OHDA-induced toxicity and acted as a scavenger of ROS, thus leading to a suppression of inflammation for which the ROS are signal molecules (22).

We further tested the protective effects of daNGOs against 6-OHDA induced toxicity *in vivo* using the well-known 6-OHDA-induced rat model of PD. The use of 6-OHDA in

these animals induces oxidative stress at mitochondrial complexes, resulting in more than 90% of dopaminergic neuronal death in a few days and also clear motor symptoms (30). In our current experiments, we found that the akinesia symptoms were improved in the daNGO group compared with the control group when we conducted a stepping test. This result suggests that daNGOs will prevent dopaminergic cell loss from 6-OHDA-induced toxicity because the stepping test is well-established method for evaluating forelimb akinesia and for predicting the extent of dopaminergic depletion (31). Stepping test scores have also been reported to be well correlated with striatal dopamine depletion (32). Furthermore, our present results from an apomorphine-induced rotation test of our PD model animals indicated a lower loss of dopaminergic neurons in the daNGO group.

By immunofluorescent staining of our experimental rats, we found that the number of TH-positive cells in the daNGO group was higher than that in the PD control group, further indicating that dopaminergic cells were preserved by exposure of these animals to the daNGOs. TH is a rate limiting enzyme of dopamine synthesis and is used as a dopaminergic neuronal marker. Iba-1 is the marker of microglial activation and inflammation. Activated microglia show an increased cell body and amoeboid shape. In the PD control group, the 6-OHDA injections induced significantly increased microglial activation compared to the daNGO group, again suggesting that the neuroprotective effects of the daNGOs resulted from their anti-inflammatory actions. All things considered, we conclude from our current findings that daNGOs have neuroprotective and preventive effects against the neurotoxicity induced by 6-OHDA on dopaminergic neurons, both *in vitro* and *in vivo*.

The most important cause of PD is the loss of dopaminergic neurons due to neuroinflammation and α-synuclein toxicity. Thus, protecting dopaminergic neurons from these toxic events could be a disease modifying treatment for PD. GO is known to inhibit the aggregation of abnormal proteins that induce neuronal cell death, and recent studies revealed

that GO reduces α-synuclein toxicity by preventing α-synuclein amyloid formation (10, 33-35). Our present study confirmed that daNGO has ROS-scavenging and anti-inflammation effects, showing its potential application for PD treatment. Our results also suggest an expanded daNGO application in other neuroinflammation-related neurodegenerative diseases, such as Alzheimer's disease, multiple sclerosis, and traumatic brain injury as well as abnormal protein aggregation-related diseases. Furthermore, daNGO could be applied to other research fields to elucidate its effects on inflammation processes that occur throughout pain, immune reactions, and degenerative changes.

MATERIALS AND METHODS

Preparation of deca nano-graphene oxide (daNGO)

daNGO preparations were provided by Biogo Co.,LTD (Seoul, Korea), and the graphene oxide was synthesized from graphite using the modified Taylor method (36). Briefly, the oxidation of bulk graphite with oxidizing agents ($KMnO_4$ and H_2SO_4) and ultrasonication were performed and the daNGOs were dispersed in deionized water. For measuring the thickness of daNGO particles, samples were prepared on a silicon wafer and measured by atomic force microscopy (AFM) (NX10; Park Systems, Suwon, Korea). Additionally, the lateral sizes of the daNGOs were analyzed by particle size analysis (PSA) (CPS Disc Centrifuge; CPS Instruments, Prairieville, Louisiana).

Cell culture

The human dopaminergic neuroblastoma SH-SY5Y cell line was obtained from KCLB (Korean Cell Line Bank, Seoul, Korea) and grown in DMEM/F-12 (Gibco, Grand Island, NY) containing 10% heat-inactivated fetal bovine serum (Gibco) and 1% (100U/ml) penicillin-streptomycin in humidified incubator with 5% CO_2 at 37°C.

MTT assay

MTT assays were performed to measure cell viability. Briefly, SH-SY5Y cells were seeded at a density of 10^5 cells per well in a 24-well culture plate (Nunc, Roskilde, Denmark), and grown to confluency. The confluent cells were treated with 6-OHDA (5-400 μM) or/and daNGO (0.3μg/ml - 300 μg/ml) for 24 h. After treatment, the cells were incubated for a further 2 h in 500 μl of MTT solution (0.25 mg/ml of fresh medium) at 37°C with 5% CO_2. The growth medium was then replaced with 500 μl of DMSO was added and incubated with shaking for 2-3 min. Absorbance of the converted dye in living cells was detected at a wavelength of 570 nm using an Infinite 200 PRO microplate reader (Tecan, Männedorf, Switzerland).

Measurement of intracellular ROS

The levels of intracellular ROS were quantified using 2′,7′-dichlorofluorescein diacetate (H2-DCF-DA, Invitrogen, Waltham, MA). DCF-DA, a non-fluorescent compound, is deacetylated by ROS within the cell into 2′,7′-dichlorofluorescein (DCF), showing green fluorescence. SH-SY5Y cells were treated with 6-OHDA (Sigma, St. Louis, MO; 10 μM) or/and daNGO (3 μg/ml) for 24 h. After washing, the cells were collected and incubated with 20 μM DCF-DA for 30 min at 37°C in 5% CO_2. The cells were then washed twice with PBS, and the relative levels of fluorescence were measured by flow cytometry on a FACSCalibur using CellQuest software (BD Biosciences, Franklin Lakes, NJ).

Experimental animals

Twenty three male Wistar rats (Orient Bio Inc., Seongnam, Korea), weighing 300–350 g at the beginning of the experiment, were housed with a 12/12 h light/dark cycle and given free

access to food and water. All of the animal procedures used in this study complied with the guidelines of the Institutional Animal Care and Use Committee of the Asan Institute for Life Sciences (Seoul, Korea).

Further details are provided in the supplementary information.

ACKNOWLEDGMENTS

This study was supported by an Asan Institute for Life Sciences Grant (2022IP0076, 2022IL0035) from Asan Medical Center, Seoul, Republic of Korea, and by the Basic Science Research Program through a National Research Foundation of Korea (NRF) grant of the Korean government (MSIT) (No. 2020R1A4A4078907).

CONFLICTS OF INTEREST

The authors declare no conflicts of interest in relation to this study.

FIGURE LEGENDS

Figure 1. Preparation and characterization of daNGOs

(A) Scheme for the preparation of daNGOs. (B) The distribution of the daNGO diameters was measured using a particle size analyzer (PSA). The following particle size distributions were observed: 99% larger than 0.0055 μm, 90% larger than 0.0066 μm, 50% larger than 0.0096 μm, 10% larger than 0.0136 μm and 1% larger than 0.0182 μm. According to CPS analysis, the highest peak was 0.0101μm (number of particles = 2.8×10^{12}). (C) A 4 μm^2 AFM image showing three daNGO spots. (D) Data from the AFM image. The A-B point indicates a height of 1.3 nm (green) and a width of 118.09 nm (red).

Figure 2. Cell viability (MTT assay) and ROS detection in SH-SY5Y cells

(A) Scheme for the SH-SY5Y cell experiments. Cell viability was assessed in the presence of 6-OHDA (5-400 μM) (B) or daNGO (0.3 ng/ml - 300 μg/ml) (C) for 24 h. (D) Co-treatment of the SH-SY5Y cells with 6-OHDA (50 μM) and daNGO (3-300 μg/ml) for 24 h. (E, F) The intracellular ROS levels in these cells are shown. DCF-DA analysis following treatment of the cells with 6-OHDA (Sigma, 10 μM) or/and daNGO (3 μg/ml) for 24 h. DCF-DA fluorescence, as a normalized median fluorescence intensity (MFI), was measured using flow cytometry (E); ***$P < 0.001$, **$P < 0.01$, and *$P < 0.05$.

Figure 3. In vivo behavioral tests

(A) Experimental timeline and (B-D) stepping tests. (B) Quantification of the number of contralateral adjusting steps. (C) Quantification of the number of ipsilateral adjusting steps. (D) The ratio of adjusting stepping tests in the number of contralateral forelimb out of the contralateral plus ipsilateral forelimb. (E, F) Apomorphine-induce rotation tests. (E) The data were expressed as averaged net (contra-ipsi) rotation per min (RPM) for 45 min. (F) The net

RPMs were expressed as 5 min intervals; ***$P < 0.001$, **$P < 0.01$, and *$P < 0.05$.

Figure 4. Confocal images of tyrosine hydroxylase (TH) and Iba-1 immunofluorescence in the rat SN. (A) PD control group. (B) daNGO group. Original magnification, 100×. (C) Quantification of the number of TH-positive cells. (D) The number of TH positive cells was expressed as a cell survival rate (ipsi/contra). (E) Quantification of the number of activated microglia in the ipsilateral SN; **$P < 0.01$ and *$P < 0.05$.

REFERENCES

1. Poewe W, Seppi K, Tanner CM et al (2017) Parkinson disease. Nature reviews Disease primers 3, 1-21
2. Fabbrini G, Brotchie JM, Grandas F, Nomoto M and Goetz CG (2007) Levodopa-induced dyskinesias. Movement disorders: official journal of the Movement Disorder Society 22, 1379-1389
3. Benabid AL (2003) Deep brain stimulation for Parkinson's disease. Current opinion in neurobiology 13, 696-706
4. Kalia LV, Kalia SK and Lang AE (2015) Disease-modifying strategies for Parkinson's disease. Movement Disorders 30, 1442-1450
5. Lotharius J and Brundin P (2002) Pathogenesis of Parkinson's disease: dopamine, vesicles and alpha-synuclein. Nat Rev Neurosci 3, 932-942
6. Jenner P (2003) Oxidative stress in Parkinson's disease. Annals of Neurology: Official Journal of the American Neurological Association and the Child Neurology Society 53, S26-S38
7. Lee B-C, Lee JY, Kim J et al (2020) Graphene quantum dots as anti-inflammatory therapy for colitis. Science advances 6, eaaz2630
8. Han J, Kim YS, Lim M-Y et al (2018) Dual roles of graphene oxide to attenuate inflammation and elicit timely polarization of macrophage phenotypes for cardiac repair. Acs Nano 12, 1959-1977
9. Bacon M, Bradley SJ and Nann T (2014) Graphene quantum dots. Particle & Particle Systems Characterization 31, 415-428
10. Kim D, Yoo JM, Hwang H et al (2018) Graphene quantum dots prevent alpha-synucleinopathy in Parkinson's disease. Nat Nanotechnol 13, 812-818
11. Jeong J-K, Lee Y-J, Jeong SY, Jeong S, Lee G-W and Park S-Y (2017) Autophagic flux induced by graphene oxide has a neuroprotective effect against human prion protein fragments. International journal of nanomedicine 12, 8143
12. Xiaoli F, Yaqing Z, Ruhui L et al (2021) Graphene oxide disrupted mitochondrial homeostasis through inducing intracellular redox deviation and autophagy-lysosomal network dysfunction in SH-SY5Y cells. Journal of Hazardous Materials 416, 126158
13. Lee BC, Lee JY, Kim J et al (2020) Graphene quantum dots as anti-inflammatory therapy for colitis. Sci Adv 6, eaaz2630
14. Ma J, Liu R, Wang X et al (2015) Crucial Role of Lateral Size for Graphene Oxide in Activating Macrophages and Stimulating Pro-inflammatory Responses in Cells and Animals. ACS Nano 9, 10498-10515
15. Yue H, Wei W, Yue Z et al (2012) The role of the lateral dimension of graphene oxide in the regulation of cellular responses. Biomaterials 33, 4013-4021
16. Markovic ZM, Jovanovic SP, Maskovic PZ et al (2019) Graphene oxide size and structure pro-oxidant and antioxidant activity and photoinduced cytotoxicity relation on three

cancer cell lines. J Photochem Photobiol B 200, 111647

17. Guo S, Bezard E and Zhao B (2005) Protective effect of green tea polyphenols on the SH-SY5Y cells against 6-OHDA induced apoptosis through ROS–NO pathway. Free Radical Biology and Medicine 39, 682-695
18. Shahriar SMS, Nafiujjaman M, An JM et al (2022) Graphene: A Promising Theranostic Agent. Adv Exp Med Biol 1351, 149-176
19. Huang C, Wu J, Jiang W, Liu R, Li Z and Luan Y (2018) Amphiphilic prodrug-decorated graphene oxide as a multi-functional drug delivery system for efficient cancer therapy. Mater Sci Eng C Mater Biol Appl 89, 15-24
20. Jiang W, Chen J, Gong C, Wang Y, Gao Y and Yuan Y (2020) Intravenous delivery of enzalutamide based on high drug loading multifunctional graphene oxide nanoparticles for castration-resistant prostate cancer therapy. J Nanobiotechnology 18, 50
21. Tabish TA and Narayan RJ (2021) Crossing the blood–brain barrier with graphene nanostructures. Materials Today
22. Mittal M, Siddiqui MR, Tran K, Reddy SP and Malik AB (2014) Reactive oxygen species in inflammation and tissue injury. Antioxidants & redox signaling 20, 1126-1167
23. Moore DJ, West AB, Dawson VL and Dawson TM (2005) Molecular pathophysiology of Parkinson's disease. Annu Rev Neurosci 28, 57-87
24. Ren C, Hu X and Zhou Q (2018) Graphene Oxide Quantum Dots Reduce Oxidative Stress and Inhibit Neurotoxicity In Vitro and In Vivo through Catalase-Like Activity and Metabolic Regulation. Adv Sci (Weinh) 5, 1700595
25. Srikanth K, Sundar LS, Pereira E and Duarte AC (2018) Graphene oxide induces cytotoxicity and oxidative stress in bluegill sunfish cells. J Appl Toxicol 38, 504-513
26. Nanda SS, An SSA and Yi DK (2015) Oxidative stress and antibacterial properties of a graphene oxide-cystamine nanohybrid. International journal of nanomedicine 10, 549
27. Wang A, Pu K, Dong B et al (2013) Role of surface charge and oxidative stress in cytotoxicity and genotoxicity of graphene oxide towards human lung fibroblast cells. Journal of Applied Toxicology 33, 1156-1164
28. Elkon H, Melamed E and Offen D (2004) Oxidative stress, induced by 6-hydroxydopamine, reduces proteasome activities in PC12 cells: implications for the pathogenesis of Parkinson's disease. J Mol Neurosci 24, 387-400
29. Xicoy H, Wieringa B and Martens GJ (2017) The SH-SY5Y cell line in Parkinson's disease research: a systematic review. Mol Neurodegener 12, 10
30. Schober A (2004) Classic toxin-induced animal models of Parkinson's disease: 6-OHDA and MPTP. Cell and tissue research 318, 215-224
31. Olsson M, Nikkhah G, Bentlage C and Bjorklund A (1995) Forelimb akinesia in the rat Parkinson model: differential effects of dopamine agonists and nigral transplants as assessed by a new stepping test. J Neurosci 15, 3863-3875
32. Miyanishi K, Choudhury ME, Watanabe M et al (2019) Behavioral tests predicting striatal

dopamine level in a rat hemi-Parkinson's disease model. Neurochem Int 122, 38-46

33. Mahmoudi M, Akhavan O, Ghavami M, Rezaee F and Ghiasi SM (2012) Graphene oxide strongly inhibits amyloid beta fibrillation. Nanoscale 4, 7322-7325
34. Ghaeidamini M, Bernson D, Sasanian N, Kumar R and Esbjorner EK (2020) Graphene oxide sheets and quantum dots inhibit alpha-synuclein amyloid formation by different mechanisms. Nanoscale 12, 19450-19460
35. Alimohammadi E, Khedri M, Miri Jahromi A, Maleki R and Rezaian M (2020) Graphene-Based Nanoparticles as Potential Treatment Options for Parkinson's Disease: A Molecular Dynamics Study. Int J Nanomedicine 15, 6887-6903
36. Park WK, Kim H, Kim T et al (2015) Facile synthesis of graphene oxide in a Couette–Taylor flow reactor. Carbon 83, 217-223

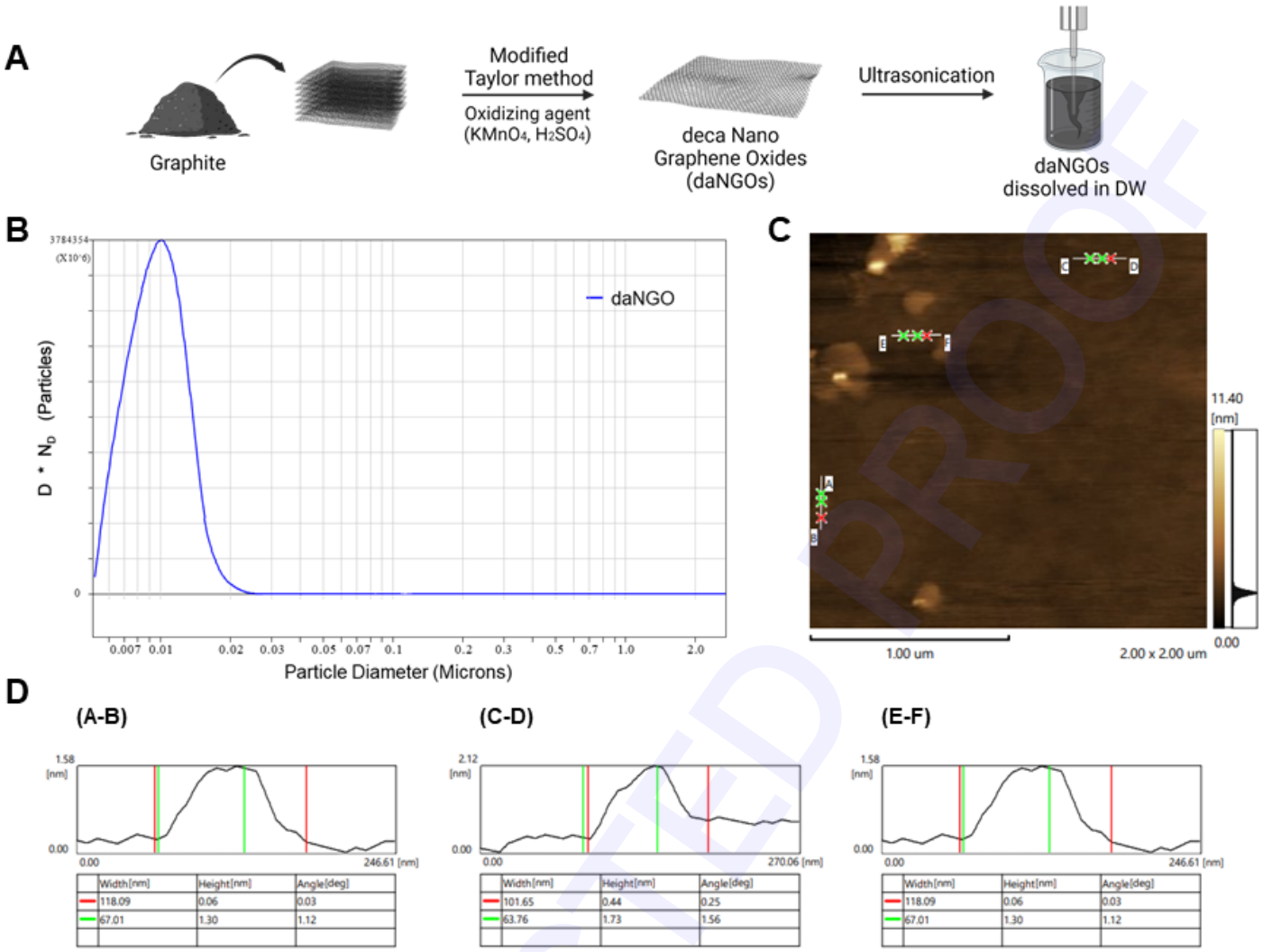

Fig. 1. Revised figure1

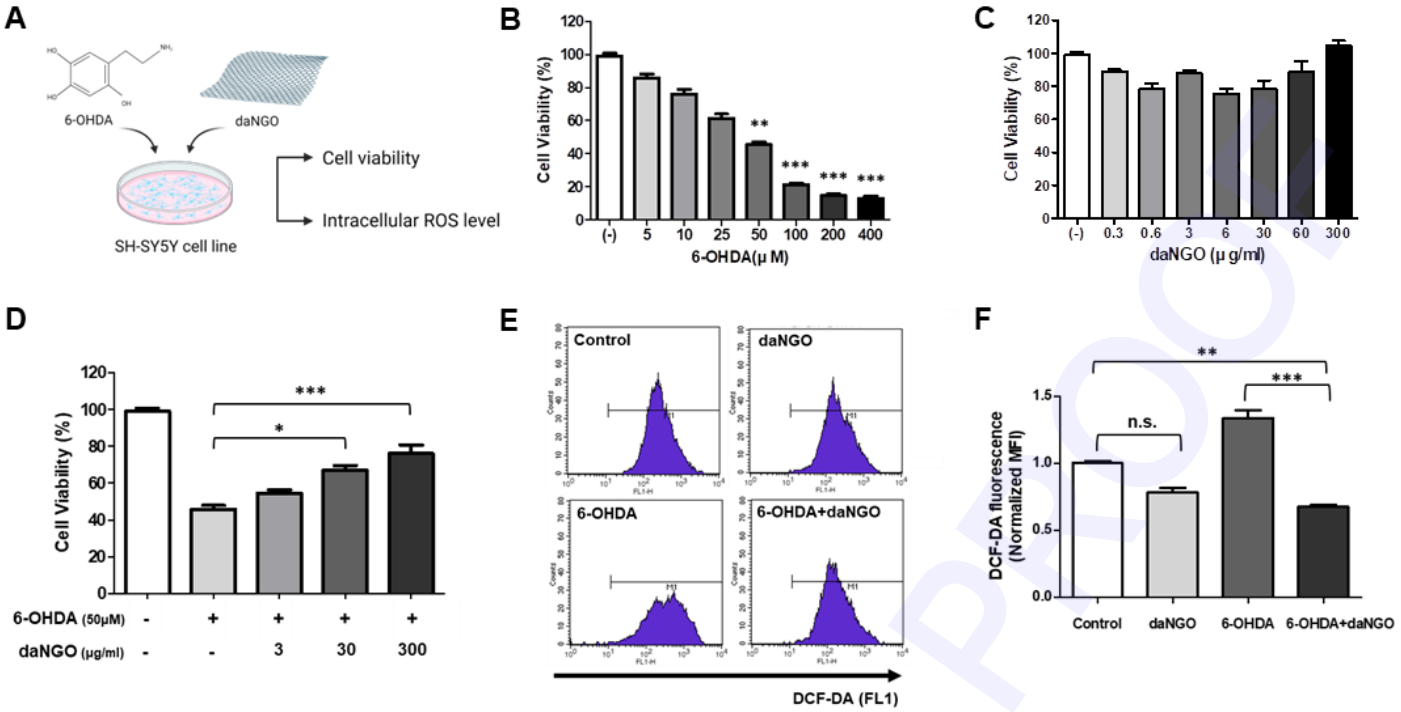

Fig. 2. Figure2

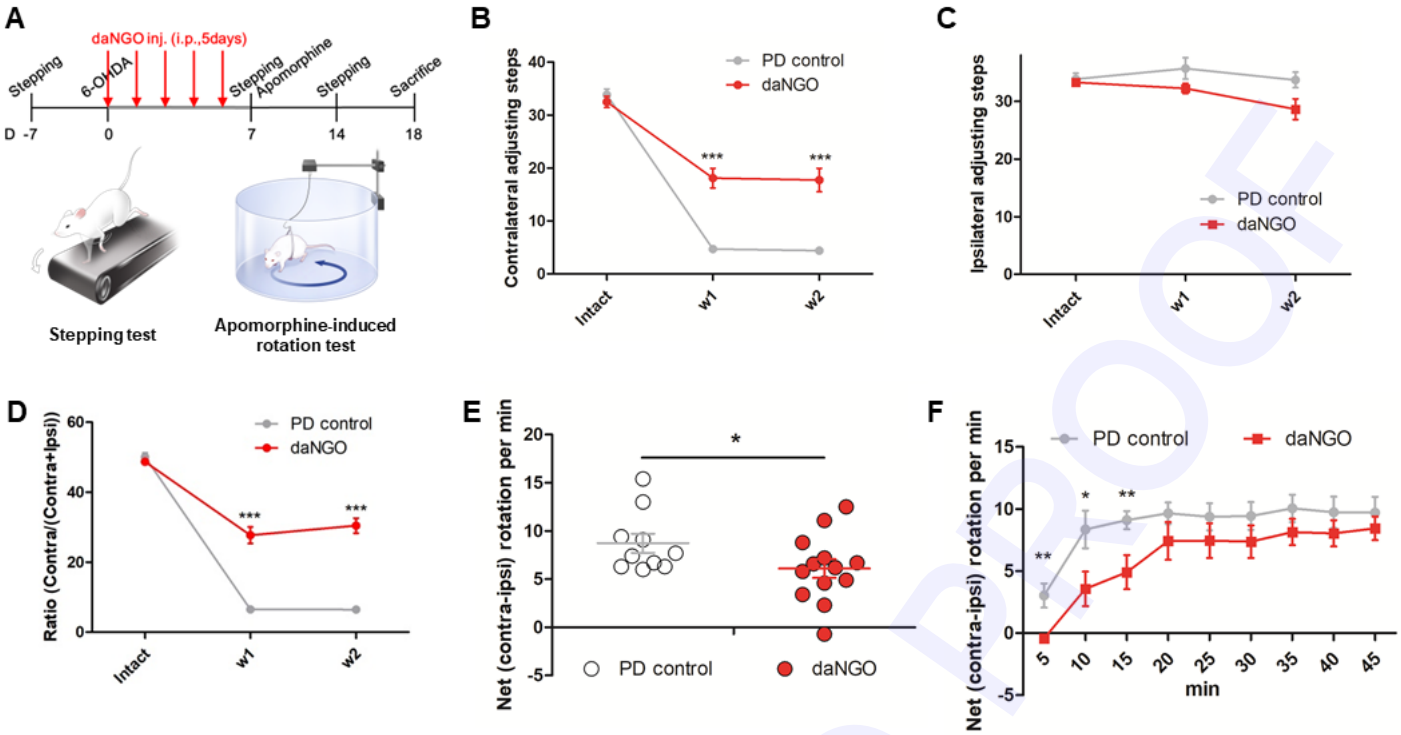

Fig. 3. Figure3

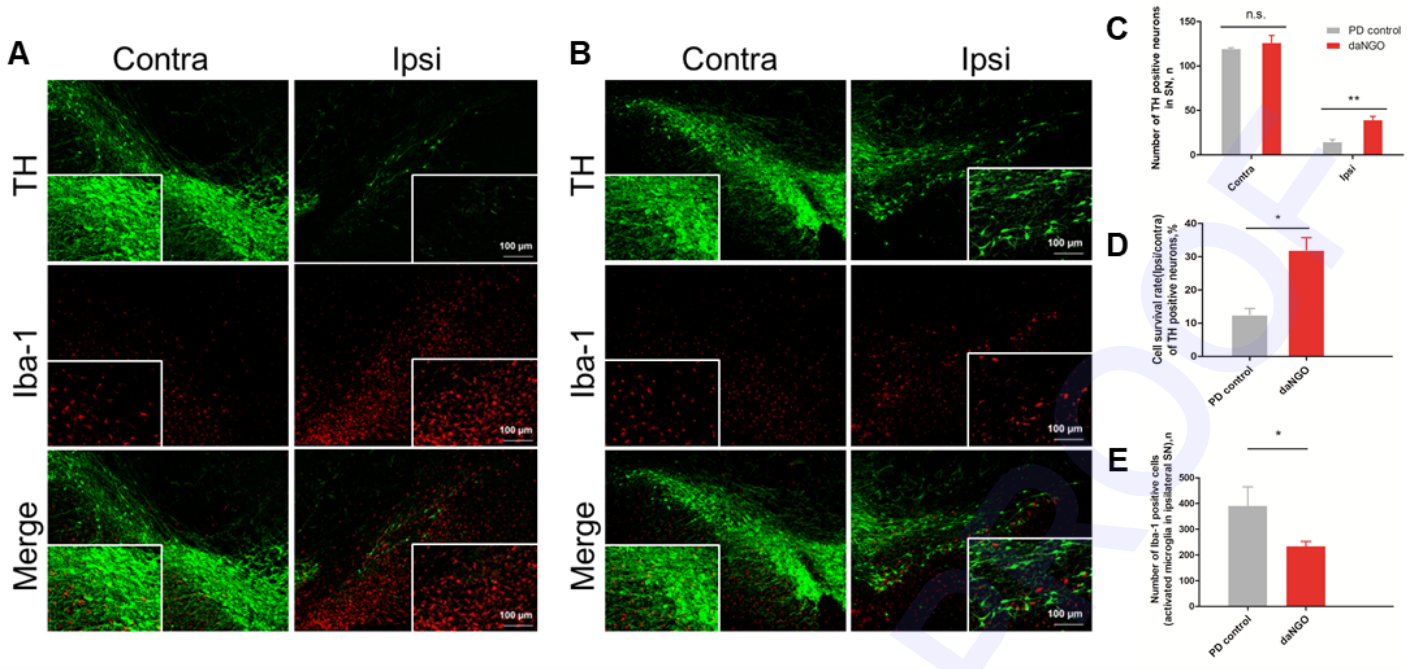

Fig. 4. Revised figure4

Supplementary information

6-OHDA lesioned rat model

General anesthesia was performed via an intraperitoneal injection of a mixture of 35 mg/kg zolazepam and tiletamine (Virbac S.A., Carros, France) plus 5 mg/kg xylazine (Bayer, Leverkusen, Germany) prior to any surgical procedures (1). Twenty three rats received a unilateral injection of 18 µg of 6-OHDA (Sigma) in 6 µL of 0.9% saline with 0.1% ascorbic acid into the medial forebrain bundle (MFB). The right MFB coordinates were AP −2.2 mm, L +1.5 mm relative to the bregma, and V −8.0 mm from the dura, with the tooth bar at +4.5 mm (1). The toxin was automatically delivered at a rate of 1 µL/min. When the injection was completed, the needle was kept in place for 5 min to prevent any back flow. The animals were then randomly separated into two groups: a PD control group (n = 10; no treatment) and daNGO group (n = 13) where each rat was subjected to a daily daNGO injection for 5 days (10 mg/ml, 30 mg/kg, i.p.).

Apomorphine-induced rotation test

Apomorphine-induced rotation tests were performed in the experimental rats at 7 days after the 6-OHDA injections. Briefly, soon after apomorphine (0.25 mg/kg; Sigma) in sterile water was injected subcutaneously, the rat was tethered to a rotometer system (Panlab, Barcelona, Spain) (1). Ipsilateral and contralateral rotations were automatically counted for 45 min. The data were expressed as the net (contralateral − ipsilateral turns) average rotations per min (RPM).

Stepping test

Stepping tests were performed as previously described (1). Briefly, while the rat's hindlimbs

and one of the forelimbs was held by the experimenter, both the contralateral and ipsilateral forelimbs were alternatively tested. The tests were performed on a moving treadmill (Jeung Do Bio & Plant Co., Seoul, Korea) at a rate of 0.18 m/s for 10 s. All experiments were video-recorded to count the number of adjusting steps. The tests were repeated twice in each session and averaged across the two trials.

Tissue processing

To fix the tissues, the rats received transcardiac perfusion with 0.9% saline containing heparin (Hanlim Pharm, Seoul, Korea), followed by 4% paraformaldehyde solution. Brain tissues were rapidly extracted and preserved in 4% paraformaldehyde for 24 h, followed by dehydration in 30% sucrose until they sank. The SN sections (AP, −4.8 to −6.0 mm, 40 μm thick) were collected using a cryostat (Leica, Wetzlar, Germany) and preserved in 0.08% sodium azide (Sigma) in PBS at 4ºC.

Immunohistochemistry

Immunohistochemistry was performed as follows. The SN sections were washed in washing buffer (0.5% bovine serum albumin in PBS) and then incubated in a blocking solution for 2 h. The sections were then washed three times and incubated with the primary antibodies indicated below overnight. After washing three times, the sections were incubated with Alexa Fluor antibodies (1:1,000; Invitrogen, Carlsbad, CA) for 2 h. The fluorescent-labeled tissues were then cover-slipped. the following primary antibodies were used: rabbit anti-TH antibody (1:1,000; Abcam, Cambridge, UK), mouse anti-TH antibody (1:2,000; Sigma), and mouse anti-Iba-1 antibody (1:300; Abcam).

Imaging and statistical analysis

Rat tissue sections were imaged using confocal microscopy (Carl Zeiss, Oberkochen, Germany) and ZEN microscope software (Carl Zeiss). All statistical analyses were conducted by Prism Software (GraphPad, La Jolla, CA). A Kruskal-Wallis test with a Dunn's post-hoc test for multiple comparisons was utilized to analyze cell viability and the DCF-DA fluorescence intensity. To analyze the differences in time-dependent patterns in the stepping tests and apomorphine-induced rotation tests, two-way repeated measures ANOVA with a Bonferroni post hoc test were conducted. The counts for the TH and Iba-1 positive cells were assessed with a Student's *t*-test. Cell intensities were quantified using the ImageJ program (NIH, Bethesda, MD). All data are presented as a mean ± standard error.

1. Yoon HH, Nam MH, Choi I, Min J and Jeon SR (2020) Optogenetic inactivation of the entopeduncular nucleus improves forelimb akinesia in a Parkinson's disease model. Behav Brain Res 386, 112551